Nested-capillary inhibited coupling silica fiber with mid-infrared transmission and low bending sensitivity at 4000 nm

Mariusz Klimczak,[1,3,*] Dominik Dobrakowski,[1,2] Amar Nath Ghosh,[3] Grzegorz Stępniewski,[1,2] Dariusz Pysz,[1] Guillaume Huss,[4] Thibaut Sylvestre,[3] Ryszard Buczyński[1,2]

[1]*Institute of Electronic Materials Technology, Glass Department, Wólczyńska 133, 01-919 Warsaw, Poland*
[2]*University of Warsaw, Faculty of Physics, Pasteura 5, 02-093 Warsaw, Poland*
[3]*Institut FEMTO-ST, CNRS, UMR 6174, Université Bourgogne Franche-Comté, Besançon, France*
[4]*LEUKOS, 37 rue Henri Giffard, Z.I. Nord, 87280 Limoges, France*
**Corresponding author: mariusz.klimczak@itme.edu.pl*

Received XX Month XXXX; revised XX Month, XXXX; accepted XX Month XXXX; posted XX Month XXXX (Doc. ID XXXXX); published XX Month XXXX

We report a silica glass nested capillary inhibited coupling fiber with transmission and low bending sensitivity in the mid-infrared around 4000 nm. The fiber is characterized in terms of transmission over 1700-4200 nm wavelengths, revealing a mid-infrared 3500-4200 nm transmission window, clearly observable for a 12 m long fiber. Bending loss around 4000 nm is 0.5 dB/m measured over 3 full turns with 40 mm radius, going up to 5 dB/m for full turns with 15 mm radius. Our results provide experimental evidence of hollow-core silica fibers in which nested, anti-resonant capillaries provide high bend resistance in the mid-infrared. This is obtained for a fiber with large core diameter of over 60 µm relative to around 30 µm-capillaries in the cladding, which motivates its application in gas fiber lasers or fiber-based mid-infrared spectroscopy of CO_x or N_xO analytes.

http://dx.doi.org/

The inhibited coupling guiding mechanism in optical fibers significantly limits the overlap of the air-core guided mode with the glass capillary structures forming the cladding. The first reported inhibited coupling fibers (ICFs) were the Kagomé fibers, developed in 2002 [1]. The principle of light guidance in such fibers was explained in 2007 [2], revealing the fundamental difference between photonic bandgap (PBG) and inhibited coupling (IC). A simplified structure, consisting of only one ring of circular capillaries of the cladding, was first reported in 2011 [3]. This was followed by a rapid development of various designs of hypocycloid-core fibers with emphasis on fibers with the core area limited by a single ring of circular, non-touching capillaries [4,5]. Low intrinsic nonlinearity and dispersion of these fibers make them particularly attractive for high energy pulse delivery [6]. The possibility to largely modify their optical properties by infiltration with liquids or gases opens up interesting applications in optofluidics [7] or temporal compression down to single optical cycles of laser pulses in the mid-infrared [8]. Low attenuation is the obvious advantage of any fiber for a practical application and loss below 10 dB/km in the visible and at important laser wavelengths in the near-infrared has been reported in ICFs [9,10]. More recently, an anti-resonant fiber with measured attenuation of 2 dB/km at a wavelength of 1512 nm made it possible to consider them for specific telecommunication applications [11]. Such applications are among the important motivations for development of hollow-core fibers and data transmission was demonstrated in an air-core photonic bandgap fiber already in 2013 [12]. Dramatic improvement in bringing down of attenuation level – ultimately down to around 1 dB/km – prompted later demonstrations of data transmission in inhibited coupling fibers in the third telecommunication window, as well [13-15]. Mid-infrared guidance in silica fibers is disruptive for gas sensing and spectroscopy applications [4,16]. The feasibility to design robust multiple-pass setups is crucial for development of fiber-based cavity-enhanced spectroscopy [17]. Several-meter or longer gas-filled fibers are becoming important for fiber-based gas lasers exploiting Raman scattering [18]. More recently, mid-infrared lasers operating between 3100 nm or 4600 nm wavelengths and based on optical transitions between vibrational energy bands of different molecular gasses, have been reported using gas-filled, anti-resonant fibers [19-22]. The fiber cavity length, exceeding 10 m in either of cases, was reported among the key parameters of optimizing the system efficiency, which puts significant pressure

on bending loss performance of fibers used to build such systems. Gas-filled ICFs have also been shown as attractive experimental platforms for nonlinear propagation, broadening and compression of ultrashort pulses across the UV to mid-infrared [23-26]. ICFs made of silica glass have been experimentally demonstrated to guide light at wavelengths up to 7900 nm, with attenuation at 3900 nm of roughly 50 dB/km [27]. Attenuation of 34 dB/km at 3050 nm and 85 dB/km at 4000 nm, was found for ICFs with a triangular cladding [28,29].

Mode confinement in ICFs is very sensitive to bending and is considered as one of the greatest challenges [30]. Hollow core PBG fibers were outperforming anti-resonant fibers in this regard [30]. Significant research effort has been devoted to overcoming this drawback, resulting in reported bend losses of ICFs in the order of 0.25 dB/turn [31], 0.2 dB/m of attenuation at 5 cm radius in the NIR range [32] and finally a result of 0.03 dB/turn bend loss for a 30 cm bend diameter at 750 nm has been reported [11]. Bend loss below 1 dB/km for R=10 cm at 1512 nm was recently demonstrated as well [11]. An important conclusion was drawn between low bending loss and small core diameter ICFs [33]. A variant of ICFs with nested capillaries has been shown to alleviate the challenge of bend losses [34]. First reported fabricated structure with nested capillaries was a 10-capillary ICF, followed by a 5-capillary fiber [35,36].

In this Letter, we report on development of an inhibited-coupling, silica glass fiber with nested capillaries, and on characterization of its transmission, attenuation and bending losses with a focus on the mid-infrared spectral range around 4000 nm.

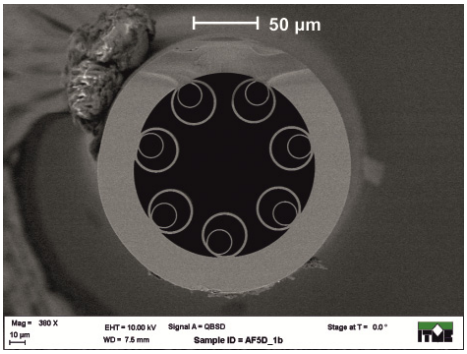

Fig. 1. SEM image of the nested capillary inhibited-coupling fiber.

The silica glass nested capillary ICF was fabricated using the stack-and-draw technique. Microstructure of the fiber is shown at a scanning electron microscopy (SEM) image in Fig. 1. It consists of a cladding with 7 nested capillaries. Criterion for number of capillaries is usually attenuation of fiber and exceptionally low attenuation has been reported for ICFs with between 5 [14,37], through 6-7 [9,30] to 8-10 capillaries [4] in the cladding. A 7-nested capillary ICF has been reported previously, albeit with significantly less uniform structure, than that in Fig. 1 [38] and nested capillary ICFs have been numerically investigated for mid-infrared transmission [39]. The outer diameter of our fiber is 162 µm, the air core diameter is 62 µm. The outer and inner capillary diameters are 29 µm and 16 µm, and their wall thickness are 1.6 µm and 0.9 µm, respectively.

All transmission measurements and mode imaging has been performed with a 150 cm long sample. Light from a Leukos Electro-250-Mir supercontinuum and NKT Photonics SuperK MIR supercontinuum has been coupled to the fiber with a mid-infrared, black diamond aspheric lens (Thorlabs C036TME). At output of the fiber, light was collimated with a parabolic off-axis silver mirror with a 10 cm focal length into a free-space input of a Fourier transform infrared (Thorlabs OSA205, FTIR) optical spectrum analyzer (OSA) for measurements in the mid-infrared or to a diffractive OSA for long-wave near-infrared measurements (Yokogawa AQ6375B). This, together with securing of both fiber ends in 9 cm long bare fiber mounts on translation stages, assured mechanical stability during measurements. In a similar way, the fiber output was collimated for characterization using an extended InGaAs beam profiler.

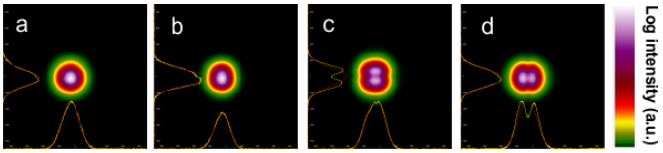

Fig. 2. Beam profiler images of fiber output recorded at 2500 nm: (a) unperturbed fundamental mode in effectively straight fiber, (b) fundamental mode when the fiber is coiled at 0.5 cm radius, (c) and (d) LP_{11} modes with the fiber is effectively straight and coiled at 0.5 cm radius, respectively.

The fiber supports guidance of few modes at 2500 nm, but the fundamental mode can be selectively excited, as shown in Fig. 2(a). Higher order modes in this case were excited using offset launch, as shown in Fig. 2(c). We also measured numerical aperture (NA) of the fiber by registering output beam profiles in far field with a phosphor-covered CCD camera. Output of single-mode laser diode operating at 1548 nm was coupled into the fiber with an aspheric lens (NA=0.25). Fundamental mode or higher order modes were selectively excited by changing the coupling conditions. Output beam size was measured at $1/e^2$ of maximum intensity. NA was calculated form the slope of linear fitting of measurement points (beam radius as a distance function) using formulas $slope = tg(\varphi)$ and $NA = sin(\varphi)$, obtaining NA = 0.037 for the fundamental mode and NA = 0.077 for a higher order mode. The fiber was protected with an acrylic coating and bending as tight as to a radius of r = 0.5 cm was possible. Depending on coupling adjustment, the LP_{11} mode could be observed, as shown in Figs. 2(c,d). Bending of fiber with these modes excited resulted in scrambling to a structure similar to the fundamental mode.

Fig. 3 contains results related to transmission and results of attenuation measurements are shown in Fig. 4. Finite element method simulation results, obtained using Comsol Multiphysics (Wave optics module) for the fiber based on a vectorized image of real fiber structure, are shown in Fig. 3(a). Triangular mesh was used in modelling with mesh elements ranging from 0.4 µm to 0.015 µm, depending on covered area of fiber structure. Material loss of silica was neglected. Bending loss was modelled assuming straight fiber geometry with modified refractive index [40]. Simulation results predict transmission windows in the 1800-2600 nm spectral range, as well as over 3400-5000 nm. Attenuation penalty of around a factor of 10 at a wavelength of about 4500 nm can be anticipated, and this is related to the fact, that equal capillary thickness has not been maintained in the technological process. Numerical simulations of bend loss further reveal, that confinement loss penalty of about 1 dB/m can be expected, regardless of bend radius, when comparing an equal capillary thickness (0.9 µm) and the developed fiber structures. Up

to the wavelength of around 4200 nm there is good agreement between the simulated and measured transmission spectra, as shown in Fig. 3(b). Compared to single capillary ring structure, simulations show that the nested capillary design would have a magnitude lower bend loss in each of the transmission windows, and similarly lower straight fiber attenuation, although straight fiber advantage would be lost closer to 5000 nm due to uneven capillary wall thickness. Simulations allow to expect transmission in the mid-infrared window to extend at least to 5000 nm, although we did not have light sources with spectral coverage above 4200 nm to verify this experimentally.

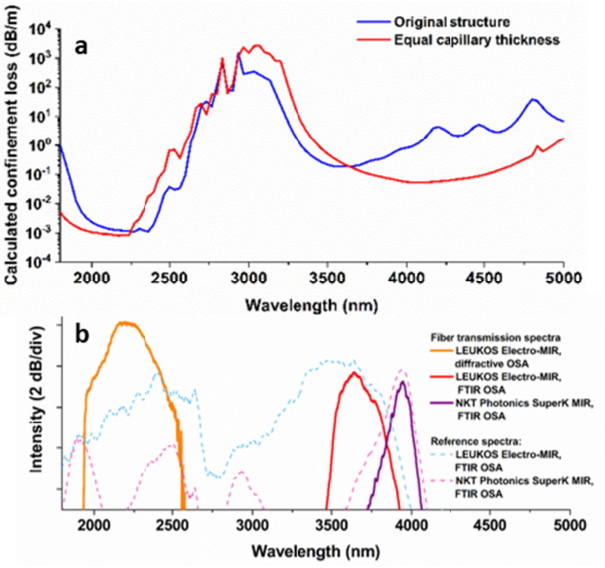

Fig. 3. (a) Finite element method-based simulation of the fiber transmission windows; (b) measured transmission spectrum for a 150 cm long fiber sample.

Attenuation of the fiber was measured by a standard cut-back method starting with a 12 m long sample. The fiber was cut by 2 m in the following measurement steps, down to 4 m of final fiber length. During the measurement, fiber was loosely looped over roughly 1 m of diameter, and no loops were made toward the end of measurement. A standard telecommunications fiber cleaver produced high-quality, repeatable cleaves and for every fiber length, the spectrum was recorded for three consecutive cleaves, to ensure measurement repeatability. Measured attenuation in the mid-infrared from around 3600 nm to 4000 nm was 1.5 dB/m and between 0.5 and 1.0 dB/m in the long-wave near-infrared, as shown in Fig. 4 (thick red traces). LP_{01} mode losses obtained in simulations are up to three orders of magnitude lower around 2400 nm and a factor of two smaller around 4000 nm. This mismatch cannot be due to inclusion of silica material loss in modelling, because calculated power fraction in glass for this fiber is between 10^{-4} to 10^{-5}. Surface scattering loss in the considered spectral range can account for 1 dB/km and does not explain the discrepancy, neither [3]. Measured attenuation level is reproduced in simulations only when contribution of higher order modes is assumed, especially that of LP_{02}. Thus we relate attenuation of the fiber to content of higher order modes, which prompts for optimization of cladding and core diameters ratio in the discussed fiber. We note that dB/km straight-fiber loss has been reported in ICFs of the single capillary or "ice-cream cone" cladding designs in similar wavelength range [9,28].

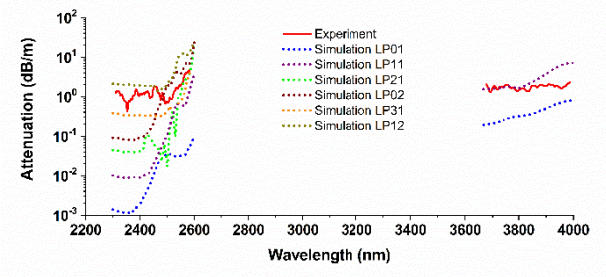

Fig. 4 Fiber attenuation measured using cut-back method starting from a 12 m long sample (solid traces) and calculated losses for different modes (dotted traces).

Bending loss measurement was performed by coiling of the 4 m long fiber sample into consecutive, full turns (full loops) of identical diameter, similarly to the procedure reported earlier for inhibited coupling fibers in [31]. Results – shown in Fig. 5 - were recorded for different bending radii from 40 mm down to 7.5 mm. In the mid-infrared window measured between 3500 and 3900 nm, the loss remains below 5 dB/m for bending radii of 15 mm or more, while for loops with radius of 30 mm or 40 mm, it remains below 2.5 dB/m down to 0.5 dB/m around 3800-3900 nm for 40 mm of bend radius. In the 1900-2600 nm window, a sharp short-wavelength transmission cut-off can be observed, which redshifts under bending with decreasing bending radius. We assign this to gradual (with decreasing bend radius) conversion of the LP_{01} mode to higher order modes, which are attenuated stronger, similarly to what was observed by authors in [28]. We note that in state-of-the-art single capillary-ring ICFs bending loss at the level of dB/km has been reported, although this related to the telecommunications wavelengths, i.e. less than 5 dB/km of loss (50 mm radius) over 1250-1650 nm [11] or over larger bending radii, i.e. 15 cm with 50 dB/km at around 3500 nm [9].

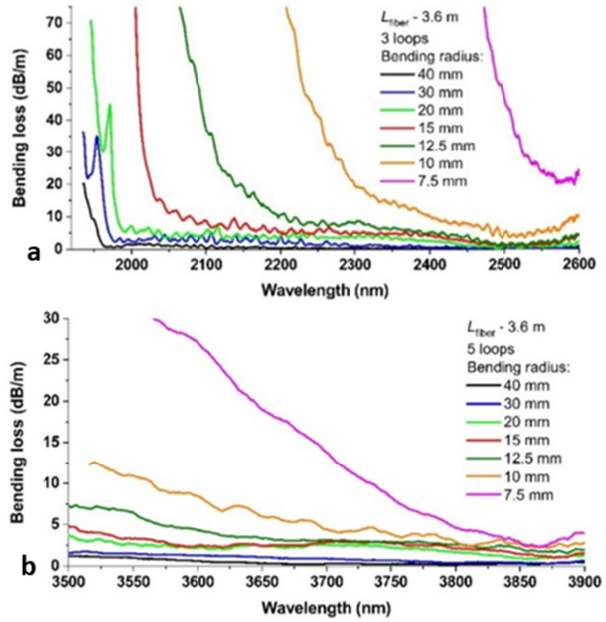

Fig. 5. Measured bend loss over three full turns for different bend radii over the long-wave near-infrared (a) and mid-infrared transmission windows of the developed ICF.

In conclusion, we reported successful development of an inhibited coupling silica fiber with mid-infrared transmission up to around 4200 nm, while numerical simulations allow to anticipate this transmission window to continue up to at least 5000 nm. This would cover frequencies of asymmetric stretching vibrational modes of CO_2 and N_2O molecules (wavelengths around 4250 nm and 4500 nm, respectively). The measured mid-infrared attenuation of 1-2 dB/m prompts for improvement of both the fiber design and the technological procedure. At the design level, the cladding capillary to the core diameter ratio should be optimized for effectively single-mode operation. Recent theoretical results reported for nested capillary ICFs identify this ratio at around 1.129 [37], while in our case it is around 0.46. At the technological level, the pending improvement relates to maintaining of similar capillary wall thickness. Despite these imperfections, already with the demonstrated fiber were we able to achieve very low bending sensitivity corresponding to bending loss down to 0.5 dB/m at a bending radius of just 40 mm at 3800-3900 nm wavelengths, by introducing nested capillaries into the fiber microstructure. We note, that exceptional results in terms of attenuation and bending loss at a single dB/km level have been reported in hollow core conjoined tube capillaries and in nested capillary nodeless ICFs, in each case in the third telecommunication window [11,14]. Tens of dB/km loss in effectively straight ICFs has been reported around 3000-4000 nm, eg. [28,29], which also identified the challenge of bend loss in this wavelength range for bending radii smaller than 20 cm. Our results provide an experimental evidence for the feasibility of limiting bending loss to reasonable levels for bend radii as small as 3-4 cm and for the crucial role of the nested anti-resonant capillaries in providing high bend loss resistance in hollow-core silica fibers operating in the mid-infrared.

Acknowledgements: The authors acknowledge following partners for lending equipment: LEUKOS (Electro-MIR), Interlab in Warsaw and NKT Photonics (SuperK MIR), prof. Ryszard Piramidowicz from Warsaw University of Technology (Yokogawa AQ6375B OSA).

Funding. Fundacja na rzecz Nauki Polskiej (FNP) (First TEAM/2016-1/1); Horizon 2020 Framework Programme (H2020) (722380); French Government and the French Embassy in Poland (2018); Région Bourgogne Franche-Comté (2018).

References

1. F. Benabid, J. C. Knight, G. Antonopoulos, and P. S. J. Russell, Science **298**, 399 (2002).
2. F. Couny, F. Benabid, P. J. Roberts, P. S. Light, and M. G. Raymer, Science **318**, 1118 (2007).
3. A. D. Pryamikov, A. S. Biriukov, A. F. Kosolapov, V. G. Plotnichenko, S. L. Semjonov, and E. M. Dianov, Opt. Express **19**, 1441 (2011).
4. F. Poletti, Opt. Express **22**, 23807 (2014).
5. C. Wei, R. Joseph Weiblen, C. R. Menyuk, and J. Hu, Adv. Opt. Photonics **9**, 504 (2017).
6. P. Jaworski, F. Yu, R. R. J. Maier, W. J. Wadsworth, J. C. Knight, J. D. Shephard, and D. P. Hand, Opt. Express **21**, 22742 (2013).
7. X.-L. Liu, W. Ding, Y.-Y. Wang, S.-F. Gao, L. Cao, X. Feng, and P. Wang, Opt. Lett. **42**, 863 (2017).
8. U. Elu, M. Baudisch, H. Pires, F. Tani, M. H. Frosz, F. Köttig, A. Ermolov, P. ST.J. Russell, and J. Biegert, Optica **4**, 1024 (2017).
9. B. Debord, A. Amsanpally, M. Chafer, A. Baz, M. Maurel, J. M. Blondy, E. Hugonnot, F. Scol, L. Vincetti, F. Gérôme, and F. Benabid, Optica **4**, 209 (2017).
10. M. Maurel, M. Chafer, A. Amsanpally, M. Adnan, F. Amrani, B. Debord, L. Vincetti, F. Gérôme, and F. Benabid, Opt. Lett. **43**, 1598 (2018).
11. S.-F. Gao, Y.-Y. Wang, W. Ding, D.-L. Jiang, S. Gu, X. Zhang, and P. Wang, Nature Commun. **9**, 2828 (2018).
12. M. N. Petrovich, F. Poletti, J. P. Wooler, A.M. Heidt, N.K. Baddela, Z. Li, D.R. Gray, R. Slavík, F. Parmigiani, N.V. Wheeler, J.R. Hayes, E. Numkam, L. Grűner-Nielsen, B. Pálsdóttir, R. Phelan, B. Kelly, John O'Carroll, M. Becker, N. MacSuibhne, J. Zhao, F.C. Garcia Gunning, A.D. Ellis, P. Petropoulos, S.U. Alam, and D.J. Richardson, Opt. Express **21**, 28559 (2013).
13. J. R. Hayes, S. R. Sandoghchi, T. D. Bradley, Z. Liu, R. Slavík, M. A. Gouveia, N. V. Wheeler, G. Jasion, Y. Chen, E. N. Fokoua, M. N. Petrovich, D. J. Richardson, and F. Poletti, J. Lightwave Technol. **35**, 437 (2017).
14. T. D. Bradley, J. R. Hayes, Y. Chen, G. T. Jasion, S. R. Sandoghchi, R. Slavik, E. N. Fokoua, S. Bawn, H. Sakr, I.A. Davidson, A. Taranta, J. P. Thomas, M. N. Petrovich, D.J. Richardson, and F. Poletti, 2018 European Conference on Optical Communication (ECOC).
15. X. Wang, D. Ge, Wei Ding, Yingying Wang, Shoufei Gao, Xin Zhang, Yizhi Sun, Juhao Li, Zhangyuan Chen, and Pu Wang, Opt. Lett. **44**, 2145 (2019).
16. F. Benabid, F. Couny, J. C. Knight, T. A. Birks & P. St J. Russel, Nature **434**, 488 (2005).
17. P. T. Marty, J. Morel, and T. Feurer, J. Light. Technol. **28**, 1236 (2010).
18. F. Couny, F. Benabid, and P. S. Light, Phys. Rev. Lett. **99**, 143903 (2007).
19. M. R. A. Hassan, F. Yu, W. J. Wadsworth, and J. C. Knight, Optica **3**, 218 (2016).
20. F. B. A. Aghbolagh, V. Nampoothiri, B. Debord, F. Gerome, L. Vincetti, F. Benabid, and W. Rudolph, Opt. Lett. **44**, 383 (2019).
21. M. Xu, F. Yu, and J. Knight, Opt. Lett. **42**, 4055 (2017).
22. M. S. Astapovich, A. V. Gladyshev, M. M. Khudyakov, A. F. Kosolapov, M. E. Likhachev, and I. A. Bufetov, IEEE Photonics Technol. Lett. **31**, 78 (2019).
23. M. S. Habib, C. Markos, O. Bang, and M. Bache, Opt. Lett. **42**, 2232 (2017).
24. M. S. Habib, C. Markos, J. E. Antonio-Lopez, and R. Amezcua-Correa, Appl. Opt. **58**, D7 (2019).
25. F. Köttig, D. Novoa, F. Tani, M. C. Günendi, M. Cassataro, J. C. Travers, and P. S. J. Russell, Nature Commun. **8**, 813 (2017).
26. A. I. Adamu, M. S. Habib, C. R. Petersen, J. Enrique Antonio Lopez, B. Zhou, A. Schülzgen, M. Bache, R. Amezcua-Correa, O. Bang, and C. Markos, Sci. Rep. **9**, 4446 (2019).
27. A. N. Kolyadin, A. F. Kosolapov, A. D. Pryamikov, A. S. Biriukov, V. G. Plotnichenko and E. M. Dianov, Opt. Express **21**, 9514 (2013).
28. F. Yu, W. J. Wadsworth, and J. C. Knight, Opt. Express **20**, 11153 (2012).
29. F. Yu and J. C. Knight, Opt. Express **21**, 21466 (2013).
30. M. Michieletto, J. K. Lyngsø, C. Jakobsen, J. Lægsgaard, O. Bang, and T. T. Alkeskjold, Opt. Express **24**, 7103 (2016).
31. W. Belardi and J. C. Knight, Opt. Express **22**, 10091 (2014).
32. S.-F. Gao, Y.-Y. Wang, X.-L. Liu, W. Ding, and P. Wang, Opt. Express **24**, 14801 (2016).
33. R. M. Carter, F. Yu, W. J. Wadsworth, J. D. Shephard, T. Birks, J. C. Knight, and D. P. Hand, Opt. Express **25**, 20612 (2017).
34. W. Belardi and J. C. Knight, Opt. Lett. **39**, 1853 (2014).
35. W. Belardi, J. Lightwave Technol. **33**, 4497 (2015).
36. A. F. Kosolapov, G. K. Alagashev, A. N. Kolyadin, A. D. Pryamikov, A. S. Biryukov, I. A. Bufetov, and E. M. Dianov, Quantum Electron. **46**, 267 (2016).
37. Md. S. Habib, J. E. Antonio-Lopez, C. Markos, A. Schülzgen, and R. Amezcua-Correa, Opt. Express **27**, 3824 (2019).
38. J. E. Antonio-Lopez, S. Habib, A. V. Newkirk, G. Lopez-Galmiche, Z. S. Eznaveh, J. C. Alvarado-Zacarias, O. Bang, M. Bache, A. Schülzgen, and R. A. Correa, 2016 IEEE Photonics Conference (IPC), pp. 402–403.
39. M. S. Habib, O. Ba ng, and M. Bache, Opt. Express **23**, 17394 (2015).
40. H. Renner, J. Light. Technol. **10**, 544 (1992).

References including titles

[1] F. Benabid, J. C. Knight, G. Antonopoulos, and P. S. J. Russell, "Stimulated Raman Scattering in Hydrogen-Filled Hollow-Core Photonic Crystal Fiber," Science 298(5592), 399-402 (2002).

[2] F. Couny, F. Benabid, P. J. Roberts, P. S. Light, and M. G. Raymer, "Generation and Photonic Guidance of Multi-Octave Optical-Frequency Combs," Science 318(5853), 1118–1121 (2007).

[3] A. D. Pryamikov, A. S. Biriukov, A. F. Kosolapov, V. G. Plotnichenko, S. L. Semjonov, and E. M. Dianov "Demonstration of a waveguide regime for a silica hollow - core microstructured optical fiber with a negative curvature of the core boundary in the spectral region > 3.5 μm," Opt. Express 19(2), 1441-1448 (2011).

[4] F. Poletti, "Nested antiresonant nodeless hollow core fiber," Opt. Express 22(20), 23807–23828 (2014).

[5] C. Wei, R. Joseph Weiblen, C. R. Menyuk, and J. Hu, "Negative curvature fibers," Adv. Opt. Photonics 9(3), 504 (2017).

[6] P. Jaworski, F. Yu, R. R. J. Maier, W. J. Wadsworth, J. C. Knight, J. D. Shephard, and D. P. Hand, "Picosecond and nanosecond pulse delivery through a hollow-core Negative Curvature Fiber for micro-machining applications," Opt. Express 21(19), 22742-22753 (2013).

[7] X.-L. Liu, W. Ding, Y.-Y. Wang, S.-F. Gao, L. Cao, X. Feng, and P. Wang "Characterization of a liquid-filled nodeless anti-resonant fiber for biochemical sensing," Opt. Lett. 42(4), 863-866 (2017).

[8] U. Elu, M. Baudisch, H. Pires, F. Tani, M. H. Frosz, F. Köttig, A. Ermolov, P. ST.J. Russell, and J. Biegert, "High average power and single-cycle pulses from a mid-IR optical parametric chirped pulse amplifier," Optica 4(9), 1024-1029 (2017).

[9] B. Debord, A. Amsanpally, M. Chafer, A. Baz, M. Maurel, J. M. Blondy, E. Hugonnot, F. Scol, L. Vincetti, F. Gérôme, and F. Benabid, "Ultralow transmission loss in inhibited-coupling guiding hollow fibers," Optica 4(2), 209-217 (2017).

[10] M. Maurel, M. Chafer, A. Amsanpally, M. Adnan, F. Amrani, B. Debord, L. Vincetti, F. Gérôme, and F. Benabid, "Optimized inhibited-coupling Kagome fibers at Yb-Nd:Yag (85 dB/km) and Ti:Sa (30 dB/km) ranges," Opt. Lett. 43(7), 1598 (2018).

[11] S.-F. Gao, Y.-Y. Wang, W. Ding, D.-L. Jiang, S. Gu, X. Zhang, and P. Wang, "Hollow-core conjoined-tube negative-curvature fibre with ultralow loss," Nature Commun. 9:2828 (2018).

[12] M. N. Petrovich, F. Poletti, J. P. Wooler, A.M. Heidt, N.K. Baddela, Z. Li, D.R. Gray, R. Slavík, F. Parmigiani, N.V. Wheeler, J.R. Hayes, E. Numkam, L. Grűner-Nielsen, B. Pálsdóttir, R. Phelan, B. Kelly, John O'Carroll, M. Becker, N. MacSuibhne, J. Zhao, F.C. Garcia Gunning, A.D. Ellis, P. Petropoulos, S.U. Alam, and D.J. Richardson, "Demonstration of amplified data transmission at 2 μm in a low-loss wide bandwidth hollow core photonic bandgap fiber," Opt. Express 21(23), 28559-28569 (2013)

[13] J. R. Hayes, S. R. Sandoghchi, T. D. Bradley, Z. Liu, R. Slavík, M. A. Gouveia, N. V. Wheeler, G. Jasion, Y. Chen, E. N. Fokoua, M. N. Petrovich, D. J. Richardson, and F. Poletti, "Antiresonant Hollow Core Fiber With an Octave Spanning Bandwidth for Short Haul Data Communications," J. Lightwave Technol. 35(3), 437-442 (2017)

[14] T. D. Bradley, J. R. Hayes, Y. Chen, G. T. Jasion, S. R. Sandoghchi, R. Slavik, E. N. Fokoua, S. Bawn, H. Sakr, I.A. Davidson, A. Taranta, J. P. Thomas, M. N. Petrovich, D.J. Richardson, F. Poletti, "Record Low-Loss 1.3dB/km Data Transmitting Antiresonant Hollow Core Fibre,"2018 European Conference on Optical Communication (ECOC)

[15] X. Wang, D. Ge, Wei Ding, Yingying Wang, Shoufei Gao, Xin Zhang, Yizhi Sun, Juhao Li, Zhangyuan Chen, and Pu Wang, "Hollow-core conjoined-tube fiber for penalty-free data transmission under offset launch conditions," Opt. Lett. 44(9), 2145-2148 (2019).

[16] F. Benabid, F. Couny, J. C. Knight, T. A. Birks & P. St J. Russel, "Compact, stable and efficient all-fibre gas cells using hollow-core photonic crystal fibre," Nature 434, 488–491 (2005)

[17] P. T. Marty, J. Morel, and T. Feurer, "All-Fiber Multi-Purpose Gas Cells and Their Applications in Spectroscopy," Journal of Lightwave Technology 28(8), 1236-2340 (2010).

[18] F. Couny, F. Benabid, and P. S. Light, "Subwatt Threshold cw Raman Fiber-Gas Laser Based on H2-Filled Hollow-Core Photonic Crystal Fiber," Physical Review Letters 99, 143903 (2007).

[19] M. R. A. Hassan, F. Yu, W. J. Wadsworth, and J. C. Knight, "Cavity-based mid-IR fiber gas laser pumped by a diode laser," Optica 3(30), 218-221 (2016).

[20] F. B. A. Aghbolagh, V. Nampoothiri, B. Debord, F. Gerome, L. Vincetti, F. Benabid, and W. Rudolph, "Mid IR hollow core fiber gas laser emitting at 4.6 μm," Optics Letters 44(2), 383-386 (2019)

[21] M. Xu, F. Yu, and J. Knight, "Mid-infrared 1 W hollow-core fiber gas laser source," Opt. Lett. 42(20), 4055-4058 (2017)

[22] M. S. Astapovich, A. V. Gladyshev, M. M. Khudyakov, A. F. Kosolapov, M. E. Likhachev, and I. A. Bufetov, "Watt-level Nanosecond 4.42-μm Raman Laser Based on Silica Fiber," IEEE Photonics Technol. Lett. 31(1), 78-81 (2019)

[23] M. S. Habib, C. Markos, O. Bang, and M. Bache, "Soliton-plasma nonlinear dynamics in mid-IR gas-filled hollow-core fibers," Opt. Lett. 42(11), 2232–2235 (2017).

[24] M. S. Habib, C. Markos, J. E. Antonio-Lopez, and R. Amezcua-Correa, "Multioctave supercontinuum from visible to mid-infrared and bend effects on ultrafast nonlinear dynamics in gas-filled hollow-core fiber," Appl. Opt. 58(13), D7-D11 (2019).

[25] F. Köttig, D. Novoa, F. Tani, M. C. Günendi, M. Cassataro, J. C. Travers, and P. S. J. Russell, "Mid-infrared dispersive wave generation in gas-filled photonic crystal fibre by transient ionization-driven changes in dispersion," Nature Commun. 8, 813 (2017).

[26] A. I. Adamu, M. S. Habib, C. R. Petersen, J. Enrique Antonio Lopez, B. Zhou, A. Schülzgen, M. Bache, R. Amezcua-Correa, O. Bang, and C. Markos, "Deep-UV to Mid-IR Supercontinuum Generation driven by Mid-IR Ultrashort Pulses in a Gas-filled Hollow-core Fiber," Sci. Rep. 9, 4446 (2019).

[27] A. N. Kolyadin, A. F. Kosolapov, A. D. Pryamikov, A. S. Biriukov, V. G. Plotnichenko and E. M. Dianov, "Light transmission in negative curvature hollow core fiber in extremely high material loss region," Opt. Express 21(8), 9514-9519 (2013).

[28] F. Yu, W. J. Wadsworth, and J. C. Knight, "Low loss silica hollow core fibers for 3–4 μm spectral region," Opt. Express 20(10), 11153–11158 (2012).

[29] F. Yu and J. C. Knight, "Spectral attenuation limits of silica hollow core negative curvature fiber," Opt. Express 21(18), 21466 (2013).

[30] M. Michieletto, J. K. Lyngsø, C. Jakobsen, J. Lægsgaard, O. Bang, and T. T. Alkeskjold, "Hollow-core fibers for high power pulse delivery," Opt. Express 24(7), 7103 (2016).

[31] W. Belardi and J. C. Knight, "Hollow antiresonant fibers with low bending loss.," Opt. Express 22(8), 10091–10096 (2014).

[32] S.-F. Gao, Y.-Y. Wang, X.-L. Liu, W. Ding, and P. Wang, "Bending loss characterization in nodeless hollow-core anti-resonant fiber," Opt. Express 24(13), 14801–14811 (2016).

[33] R. M. Carter, F. Yu, W. J. Wadsworth, J. D. Shephard, T. Birks, J. C. Knight, and D. P. Hand, "Measurement of resonant bend loss in anti-resonant hollow core optical fiber," Opt. Express 25(17), 20612–20621 (2017).

[34] W. Belardi and J. C. Knight, “Hollow antiresonant fibers with reduced attenuation,” Opt. Lett. 39(7), 1853-1856 (2014).
[35] W. Belardi, "Design and Properties of Hollow Antiresonant Fibers for the Visible and Near Infrared Spectral Range," Journal of Lightwave Technology 33(21), 4497–4503 (2015).
[36] A. F. Kosolapov, G. K. Alagashev, A. N. Kolyadin, A. D. Pryamikov, A. S. Biryukov, I. A. Bufetov, and E. M. Dianov, "Hollow-core revolver fibre with a double-capillary reflective cladding," Quantum Electron. 46(3), 267–270 (2016).
[37] Md. S. Habib, J. E. Antonio-Lopez, C. Markos, A. Schülzgen, and R. Amezcua-Correa, “Single-mode, low loss hollow-core anti-resonant fiber designs,” Opt. Express 27(4), 3824-3836 (2019).
[38] J. E. Antonio-Lopez, S. Habib, A. V. Newkirk, G. Lopez-Galmiche, Z. S. Eznaveh, J. C. Alvarado-Zacarias, O. Bang, M. Bache, A. Schülzgen, and R. A. Correa, "Antiresonant hollow core fiber with seven nested capillaries," in 2016 IEEE Photonics Conference (IPC) (2016), pp. 402–403.
[39] M. S. Habib, O. Ba ng, and M. Bache, "Low-loss hollow-core silica fibers with adjacent nested anti-resonant tubes," Opt. Express 23, 17394–17406 (2015).
[40] H. Renner, "Bending losses of coated single-mode fibers: a simple approach," J. Light. Technol. 10(5), 544–551 (1992).